

# VLBI Collimation Tower Technique for Time-Delay Studies of a Large Ground Station Communications Antenna

T. Y. Otoshi

Radio Frequency and Microwave Subsystems Section

L. E. Young

Tracking Systems and Applications Section

W. V. T. Rusch

Department of Electrical Engineering  
University of Southern California

*A need for an accurate but inexpensive method for measuring and evaluating time delays of large ground antennas for VLBI applications motivated the development of the collimation tower technique described in this article. This article discusses supporting analytical work which was performed primarily to verify time delay measurement results obtained for a large antenna when the transmitter was at a collimation distance of 1/25 of the usual far-field criterion. Comparisons of theoretical and experimental results are also given.*

## I. Introduction

As accuracies of Very Long Baseline Interferometry (VLBI) systems for the measurement of time delay changes have continued to improve to current levels of less than 0.1 ns, a need has existed for studies to be made of accuracy-limiting errors associated with the microwave antenna itself. Two types of VLBI errors attributed to the antenna are (1) errors produced by unwanted multiple reflections (multipath signals) within the antenna propagation media and (2) undesired phase delay changes produced when the antenna is mispointed from boresight of the radio source.

The subject of antenna time delay and errors contributed by multipath signals has been studied in recent years both analytically and experimentally (Refs. 1–3). Results of studies made on some types of Deep Space Network (DSN) antennas tend to show that multipath problems can be mitigated by increasing the VLBI spanned bandwidth.

The second type problem, which is concerned with phase delay errors due to antenna mispointing, is one to which little attention has been given in the past. This subject is important because antenna mispointing can occur in practice due to intentional mispointing as in the case of consscanning VLBI systems, or unintentionally due to practical limitations on the accuracies of antenna pointing systems. Although some far-field VLBI antenna mispointing experiments have been performed with a 64-m DSN antenna, poor reproducibility of the results and insufficient experimental data have thus far prevented any definite conclusion to

be drawn concerning the effects of antenna mispointing on VLBI time delay data. There has been a strong need for quite some time now for a rigorous theoretical analysis to help predict the order of magnitude of phase delay changes that can occur for various VLBI type antennas when the mainbeam is pointed off the boresight coordinates of the radio source.

This article is concerned with supporting analytical work which was performed primarily to verify time delay measurement results obtained for a large antenna when the transmitter was at a collimation distance of 1/25 of the usual far-field criterion. The unexpected spinoff from this work was that since a collimation tower geometry is basic to many experimental configurations, the same theoretical equations can also be used to study phase delay changes as a function of antenna pointing offset angles from boresight. The analysis is applicable, not only for near-field but also for far-field studies.

## II. Theory

Application of the Lorentz Reciprocity Theorem yields the voltage coefficient of mutual coupling between two lossless, matched antennas to be (Ref. 4):

$$S_{12} = \frac{e^{j\Phi}}{4\sqrt{P_1 P_2}} \int_S (\bar{E}_1 \times \bar{H}_2 - \bar{E}_2 \times \bar{H}_1) \cdot \hat{n} dS \quad (1)$$

where  $\Phi$  is an arbitrary phase reference,  $(\bar{E}_1, \bar{H}_1)$  and  $(\bar{E}_2, \bar{H}_2)$  are the transmitted fields of each antenna,  $P_1$  and  $P_2$  are the radiated powers, and  $S$  completely encloses one of the antennas. This statement of Robieux's Theorem can be rewritten

$$S_{12} = \frac{e^{j\Phi} \int_S (\bar{E}_1 \times \bar{H}_2 - \bar{E}_2 \times \bar{H}_1) \cdot \hat{n} dS}{4 \left[ \frac{1}{2} \operatorname{Re} \int_{A_1} (\bar{E}_1 \times \bar{H}_1^*) \cdot \hat{n} dS \right]^{1/2} \left[ \frac{1}{2} \operatorname{Re} \int_{A_2} (\bar{E}_2 \times \bar{H}_2^*) \cdot \hat{n} dS \right]^{1/2}} \quad (2)$$

which, when squared, yields

$$\frac{P_R}{P_T} = |S_{12}|^2 = \frac{\frac{1}{4} \left| \int_S (\bar{E}_1 \times \bar{H}_2 - \bar{E}_2 \times \bar{H}_1) \cdot \hat{n} dS \right|^2}{\left[ \operatorname{Re} \int_{A_1} (\bar{E}_1 \times \bar{H}_1^*) \cdot \hat{n} dS \right] \left[ \operatorname{Re} \int_{A_2} (\bar{E}_2 \times \bar{H}_2^*) \cdot \hat{n} dS \right]} \quad (3)$$

In the event that one or both of the antennas does not have a clearly defined aperture, Eq. (1) can be rewritten

$$S_{12} = \frac{e^{j\Phi}}{4\sqrt{P_1 P_2}} \int_V (-\bar{E}_2 \cdot \bar{J}_1 + \bar{E}_1 \cdot \bar{J}_2) dV \quad (4)$$

where  $\bar{J}_1$  and  $\bar{J}_2$  are the source currents completely enclosed by  $S$  and  $\hat{n}$  (in Eq. 1) points *out* of  $V$ .

As a relatively simple application of Eqs. (1)-(4), consider a paraboloid and an on-axis electric dipole (Fig. 1). The paraboloid is fed by a focused, point-source feed located at its focus. The fields of the feed are

$$\bar{E}_f = V_0 e^{-j\beta L} \frac{e^{-jk\rho}}{\rho} \left( \frac{2F}{1 + \cos \theta_f} \right) (\hat{a}_{\theta_f} \cos \phi_f - \hat{a}_{\phi_f} \sin \phi_f). \quad (5)$$

Located at  $P(0, 0, R)$  on the Z-axis is an electric dipole  $\hat{a}_I d$ . Application of Eq. (4) over the paraboloid aperture then yields

$$\frac{P_R}{P_T} = \frac{G_d G_p}{\left(\frac{4\pi R}{\lambda}\right)^2} \quad (6)$$

where the dipole gain is

$$G_d = 1.5 \quad (7a)$$

and the Fresnel-region gain of the paraboloid is

$$G_p = \left(\frac{\pi D}{\lambda}\right)^2 \left\{ \frac{\sin [k(D/2)^2/4R]}{[k(D/2)^2/4R]} \right\}^2 \quad (7b)$$

where  $D$  is the paraboloid diameter.

Equations (1)–(3) can be applied to the problem of coupling between two paraboloids (Fig. 2):

- (1) Test paraboloid #1 is a large reflector with a point-source feed located at its focus. The feed pattern consists of arbitrary E- and H-plane patterns. Central blocking is included, but strut blocking is not. This reflector lies in the far-field of paraboloid #2.
- (2) Collimation paraboloid #2 is a smaller reflector with an axially-defocussed point-source feed. Various feed patterns may be specified. Central blocking is included, but strut blocking is not. This reflector need not lie in the far-field of paraboloid #1, and it can be oriented arbitrarily with respect to #1.

Voltage coupling between the two reflectors is computed by means of Eq. (1) and the corresponding power coupling by means of Eq. (3). The integration surface  $S$  is a large coaxial circle located in front of paraboloid #1 and perpendicular to its axis. This surface is generally near to #1 and sufficiently large that the fields  $\bar{E}_1$  and  $\bar{H}_1$  are assumed to be negligible beyond the limits of the circle. In principle,  $S_{12}$  should be independent of the location of this surface; in practice the size and location of the circle must be determined empirically. The fields  $\bar{E}_1$  and  $\bar{H}_1$  on  $S$  are determined by geometrical optics and geometrical edge diffraction (Refs. 5, 6).

The integration surface  $S$  is assumed to lie in the far-field of collimation paraboloid #2 so that the fields of this antenna may be expressed:

$$\bar{E}_2 = \frac{e^{-jkR}}{R} [E_{2a}(\theta_{2a}) \cos \phi_{2a} \hat{a}_{\theta_{2a}} - H_{2a}(\theta_{2a}) \sin \phi_{2a} \hat{a}_{\phi_{2a}}] \quad (8)$$

which can be decomposed into rectangular components  $E_{2x}$ ,  $E_{2y}$ ,  $H_{2x}$ , and  $H_{2y}$  for integration in Eqs. (1) and (3). The above formulations are contained in an appropriate computer program.

Provision is also made to rotate paraboloid #1 (Fig. 3) about an offset azimuth axis ( $\Delta z_{az}$ ) and an offset elevation axis ( $\Delta x_{e1}$ ,  $\Delta z_{e1}$ ). In the rotated coordinate system the integration surface  $S$  rotates with #1 so that it remains symmetrically positioned on a plane normal to the axis of #1. However, it is no longer symmetric or normal with respect to the line between #1 and #2.

### III. Experimental Setup

Figure 4 shows a block diagram of the collimation tower experimental setup for time delay measurements using VLBI measurement techniques and associated equipment. At the collimation tower, a simulated VLBI radio source signal, provided by a broadband noise source, is fed into a power divider. One of the power divider outputs is a transmit-reference signal which is recorded

on a magnetic tape recorder simultaneously with clock signals furnished by a portable rubidium frequency standard. The other power divider output is fed to the collimation tower transmitter antenna which is 1.83 m (6 ft) in diameter. The signal is transmitted over a distance of about 1.6 km and illuminates both a 1.83-m (6-ft) antenna and a 26-m (85-ft) antenna. The smaller antenna is a receive-reference antenna whose time delay (including feed and interconnecting transmission lines) has been pre-calibrated while the 26-m antenna is the antenna whose delay is being measured.

For this test, the center frequency was 8.440 GHz and the VLBI spanned bandwidth 40 MHz. When boresighted to each other, the distances between the focal points of the transmit and receive antennas were approximately  $0.08 D^2/\lambda$  and  $16 D^2/\lambda$ , respectively, for the 26-m and 1.83-m receive antenna paths where  $D$  corresponds to the applicable receive antenna diameter and  $\lambda$  is the free space wavelength. Figure 5 shows the collimation tower at DSS 13 and the 1.83-m transmit antenna used in the test, while Fig. 6 shows the 26-m antenna (being calibrated) and the receive-reference 1.83-m antenna referred to in this article.

The experimental procedure was to first record the received signal for a duration of 2 minutes for the receive-reference antenna and then switch to the 26-m antenna under test and record its received signal for 2 minutes and then switch back to the reference antenna. This procedure was repeated for a period of 1 hour during which the downconverted received signals were recorded on magnetic tape. Simultaneously recorded were clock signals provided by the station hydrogen maser frequency standard.

The recorded data was later postprocessed on the Caltech-JPL VLBI correlator where received signal recordings were correlated against the transmit-reference signal data recorded at the collimation tower. The final experimental value was determined after correcting the VLBI correlator output data for the precalibrated delays of the receive-reference antenna and all interconnecting transmission lines and waveguides of the receive-reference antenna and the 26-m antenna up to the common switching port.

The advantages of switching between a reference antenna and the antenna under test is that common modes changes such as propagation media changes, multipath, and system drifts tend to cancel out. It is reasonable to expect that better accuracy and precision can be obtained from comparisons made with a calibrated delay standard than from direct absolute delay measurement over long distances.

#### IV. Comparisons of Theoretical and Experimental Data

The basic theory of antenna time delay for Cassegrain antennas has been discussed in Ref. 1. To compute the theoretical value of antenna delay for the results of this paper, the output phase of integrated fields received by the antenna is computed at the two microwave frequencies involved in the VLBI experiment (resolving any multiples of  $2\pi$  radian ambiguities). Then group delay is computed by the "VLBI bandwidth synthesis" equation (Ref. 7) which is equivalent to the "phase-slope" method of determining group delay (Ref. 8).

One of the significant results of this experiment was that a measurement precision of 10 ps (corresponding to 0.3 cm) was achieved. A second important result was that a significant difference was found between the theoretical 26-m antenna delay determined from mutual coupling theory and the value calculated from the optical ray pathlength of a single ray traveling from the collimation tower antenna to the feed horn phase center of the 26-m antenna. The near-field delay, based on mutual coupling theory described in Section II of this article, was calculated to be 0.6 ns longer than the value determined from the ray optical pathlength calculation. A third significant result was that the experimentally determined delay of the 26-m antenna agreed with the mutual coupling theoretical value to within  $0.2 \pm 0.2$  ns probable error. The agreement between mutual coupling near-field and experimental results is excellent when taking into consideration the relatively small VLBI spanned bandwidth of the 40 MHz that was used in the experiment.

It should be pointed out that the ray pathlength calculation method is only approximately valid for a focused antenna and at far-field distances, but is a method commonly used erroneously for near-field geometries as well. The mutual coupling theoretical result is based on numerical integrations over the entire 26-m-dia. aperture using subreflector pattern data (Ref. 9) applicable to the X-band feed system that was installed on the 26-m Cassegrain antenna during the experiments. Since the subreflector pattern is referenced to the focal point of the paraboloid, it is applicable to the theory and computer program described in this paper.

Many collimation tower test setups are plagued with ground multipath problems. However, a previous study made by the Howland Co. of Atlanta, Ga., showed that for the particular ground terrain involved in this collimation tower setup and with the receive-reference antenna mounted on top of the 26-m antenna as shown in Fig. 6, ground reflected multipath signals would not interfere with accurate measurements of the delays of the two receive antennas. In addition, independent time delay measurements made on the 26-m antenna with a time domain technique similar to the FM/CW technique described in Ref. 10 confirm the VLBI results discussed in this paper. With the time domain technique, it was possible to identify and separate out the ground multipath signals and measure the delay of the primary signal accurately. Although time domain techniques can also be used to measure time delays, the FM/CW instrumentation is primarily a diagnostics tool and is not part of the standard DSN instrumentation.

Figure 7 shows a plot of power pattern for an elevation angle scan for a test frequency of 8.420 GHz and at the collimation tower geometry and distances described above for the transmit 1.83-m antenna and the receive 26-m antenna. Both theoretical and experimental data are shown. The theoretical pattern is based on uniform illumination of the 26-m antenna aperture. Later comparisons will be made where the theoretical pattern is based on subreflector pattern data (Ref. 9). The experimental data was interpolated from a linear power pattern recording which had dB calibration marks provided through the use of a rotary vane attenuator in series with the transmitter waveguide. Since the data had to be extracted from the linear power recordings, it is estimated that the experimental data shown in Fig. 7 is accurate to only  $\pm 0.5$  dB above  $-6$  dB,  $\pm 1.0$  dB between  $-6$  dB and  $-10$  dB, and  $\pm 1.5$  dB below  $-10$  dB. It is significant to note in the power pattern that both experimental and theoretical results show three bumps on the main beam. Also note that the main beam beamwidths between the  $-10$  dB points are close to  $0.8$  degree for both mutual coupling theory and experimental results at this near-field distance of  $0.08 D^2/\lambda$ . For comparison purposes, when the separation of the transmit antenna and the 26-m receive antenna changes from this near-field distance to far-field distances, the beamwidth between  $-10$  dB points changes from the  $0.8$  deg value to about  $0.15$  deg. This far-field beamwidth value was determined by performing numerical integration of the X-band subreflector pattern over the 26-m antenna aperture at 8.420 GHz and computing far-field patterns.

Also of interest is the value of  $P_{R1}/P_{T2}$  calculated from mutual coupling theory (Eq. 3) as compared to the value calculated from Friis transmission loss formula (Ref. 11). For the near-field collimation tower distance involved in the experiment, the 26-m antenna received power level was calculated from mutual coupling theory (and use of Ref. 9 subreflector data) to be smaller than the received power calculated from the Friis formula by  $13.6$  dB. The experimentally measured received power was less than the Friis value by  $13.5 \pm 1.5$  dB. The large uncertainty associated with the measured value is due to uncertainty in the efficiency of the large antenna at 8.420 GHz during earlier installation periods, and uncertainty as to whether the receive and transmit antennas were optimally boresighted to each other at the particular time of this measurement. Despite the large uncertainty in this particular experimental result, it is significant that the agreement with the mutual coupling theoretical value is still quite good.

At the time that initial boresighting and power measurements were being made, it was thought that the large difference between actual received power and the value based on Friis formula was a major experimental leakage problem. Had the theoretical results of this article been available prior to this measurement, a greater understanding of the near-field measurement procedure would have been available and greater care would have been exercised in boresighting procedures. Termination of funding for this work and recent conversion to an updated feedcone at DSS 13 make it difficult to repeat this series of experiments in the near future.

If at some time in the future, funding does become available, it would be of great interest and value to the DSN to perform additional experimental measurements with the collimation tower technique and make accurate comparisons to theory, especially with regards to studying phase delay change vs offset from boresight angles.

## V. Conclusion

This article has described the development of theoretical equations specifically developed for practical collimation tower test setup geometries. A brief description has been given of the VLBI collimation tower technique that was used for the measurement of antenna delay. An agreement of  $0.2$  ns was obtained between theoretical and experimental values of time delay for the DSS 13 26-m antenna at a collimation tower distance that was  $1/25$  the accepted  $2D^2/\lambda$  far-field criterion. These results apply to measurements performed with VLBI equipment at 8.440 GHz and 40 MHz spanned bandwidth.

Based on the results presented in this article, one can conclude that the collimation tower technique has the potential of being very useful for checkout and diagnostics of the performance of a large ground station antenna. Now that the necessary theoretical equations are available, theoretical values calculated for actual near-field geometries can be used as a criterion for expected performance. Once the near-field performance of an antenna is verified experimentally, then transformations can be made on the near-field data to predict performance in the far-field.

## Acknowledgments

The VLBI collimation tower technique described in this article was suggested by Hugh Fosque of NASA. Measurements of received power vs elevation angle were made by Juan Garnica of Bendix Field Engineering Corporation.

## References

1. Cha, A. G., Rusch, W. V. T., and Otoshi, T. Y., "Microwave Delay Characteristics of Cassegrainian Antennas," *IEEE Trans. on Antennas and Propagation*, Vol. AP-26, pp. 860-865, November 1978.
2. Otoshi, T. Y., and Rusch, W. V. T., "Multipath Effects on the Time Delays of Microwave Cassegrainian Antennas," *IEEE 1980 International Symposium Digest - Antennas and Propagation*, Volume II, 80, CH 1557-8AP, pp. 457-460, June 1980.
3. Otoshi, T. Y., and Young, L. E., "An Experimental Investigation of the Changes of VLBI Time Delays Due to Antenna Structural Deformations," *TDA Progress Report 42-68*, pp. 8-16, Jet Propulsion Laboratory, Pasadena, Calif., April 15, 1982.
4. Ludwig, A. C., "Fundamental Relationships of Electromagnetics," Technical Report NB 121, Electromagnetics Institute, Technical University, Denmark, pp. 36-42, June 1979.
5. Lee, S. W., "Uniform Asymptotic Theory of Electromagnetic Edge Diffraction," *Electromagnetic Scattering*, P.L.E. Uslenghi, editor, Academic Press, pp. 67-119 1978.
6. Rusch, W. V. T., "Antenna Notes," Technical Report NB84b, Electromagnetics Institute, Technical University, Denmark, pp. 135-140, Aug. 1974.
7. Molinder, J. I., "A Tutorial Introduction to Very Long Baseline Interferometry (VLBI) Using Bandwidth Synthesis," *DSN Progress Report 42-46*, Jet Propulsion Laboratory, Pasadena, Calif., pp. 16-28, Aug. 15, 1978.
8. Otoshi, T. Y., and Beatty, R. W., "Development and Evaluation of a Set of Group Delay Standards," *IEEE Trans. on Instrumentation and Measurement*, Vol. IM-25, No. 4, pp. 335-342, December 1976.
9. Williams, W., Nixon, D., Reilly, H., Withington, J., and Bathker, D., "A Prototype DSN X-S Band Feed: DSS 13 Application Status (Third Report)," *DSN Progress Report 42-52*, Jet Propulsion Laboratory, Pasadena, Calif., pp. 51-60, Aug. 15, 1979.
10. Otoshi, T. Y., "An FM/CW Method for the Measurement of Time Delays of Large Cassegrainian Antennas," *TDA Progress Report 42-66*, Jet Propulsion Laboratory, Pasadena, Calif., pp. 49-59, Dec 15, 1981.
11. Friis, H. T., "A Note on a Simple Transmission Formula," *Proc. IRE*, Vol. 34, pp. 254-256, May 1946.

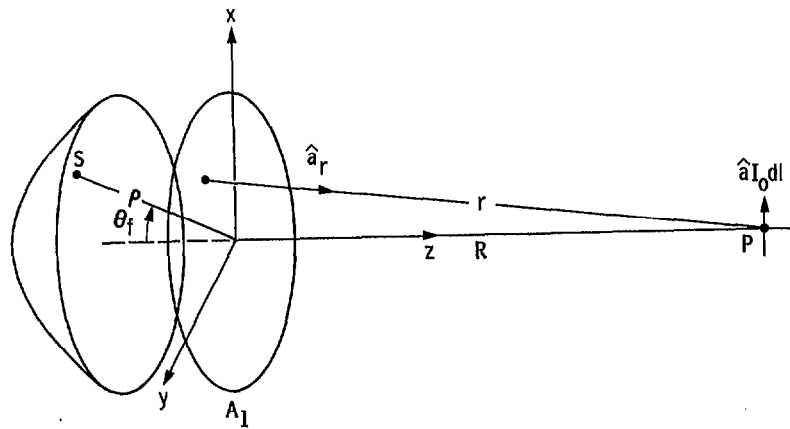


Fig. 1. Coupling between paraboloid and on-axis electric dipole

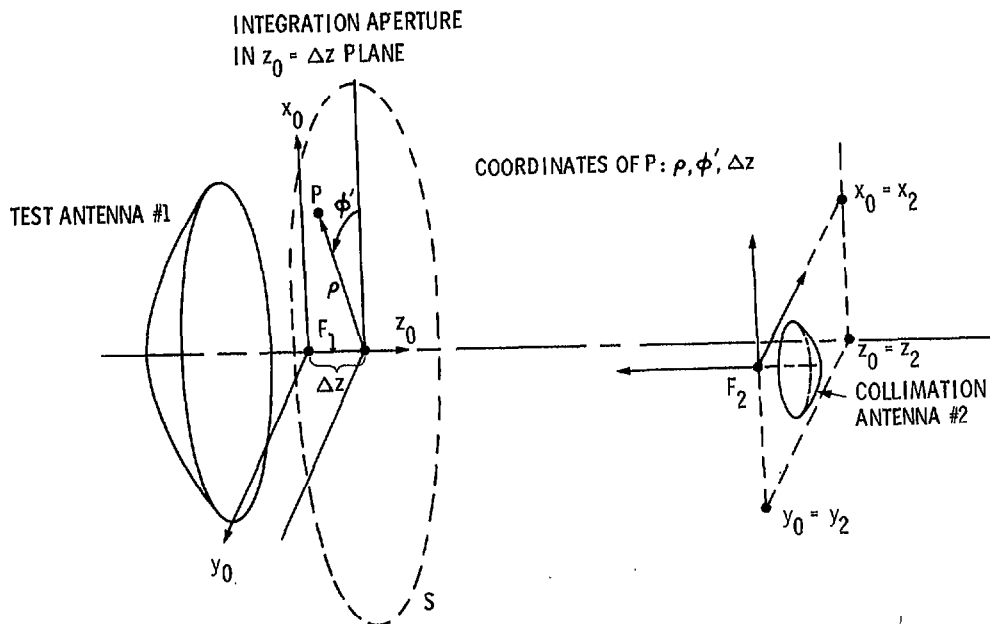
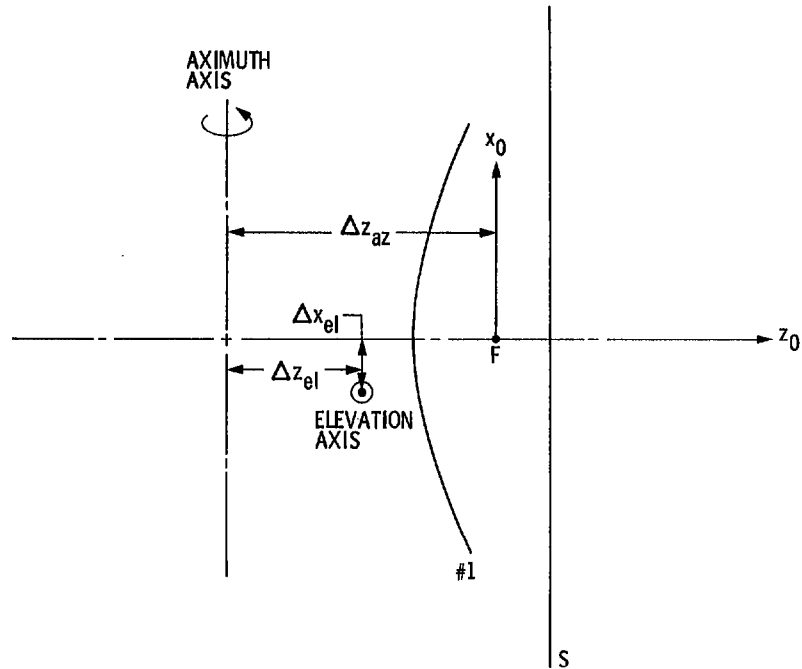
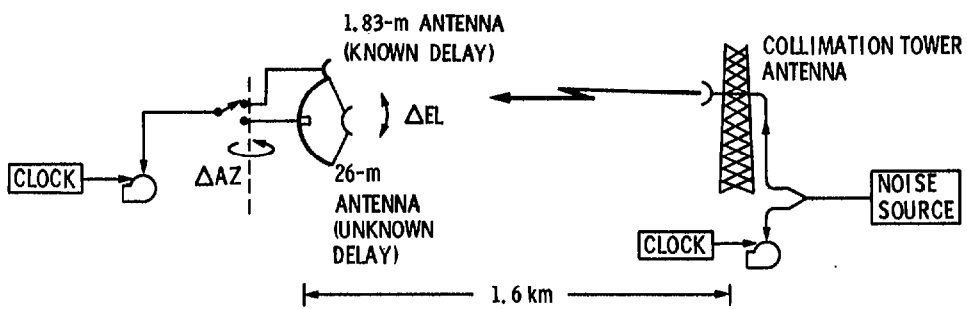


Fig. 2. Coupling geometry for two paraboloids



**Fig. 3. Geometry of Az-EI rotation**



**Fig. 4. Collimation tower geometry for the measurement of antenna time delay using VLBI technique and instrumentation**



Fig. 5. DSS 13 collimation tower and 1.83-m (6-ft) diameter transmit antenna. The S-band feed shown in photograph was replaced by an X-band feed

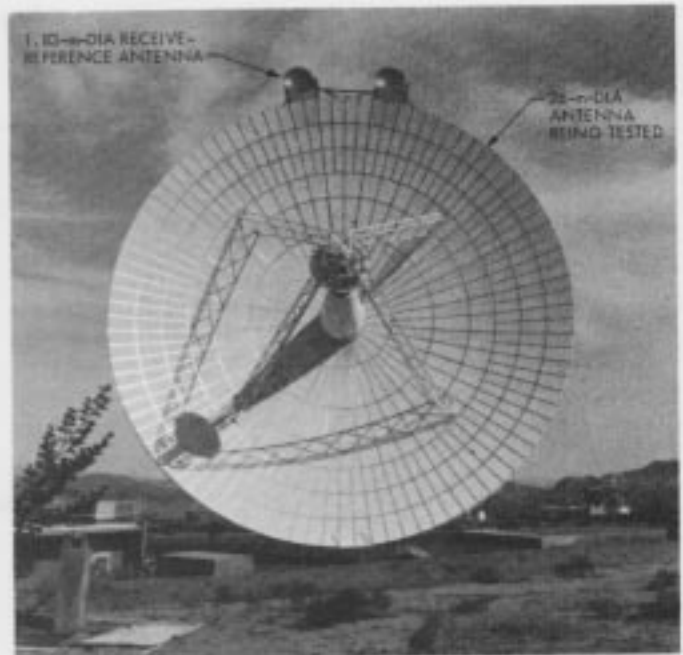
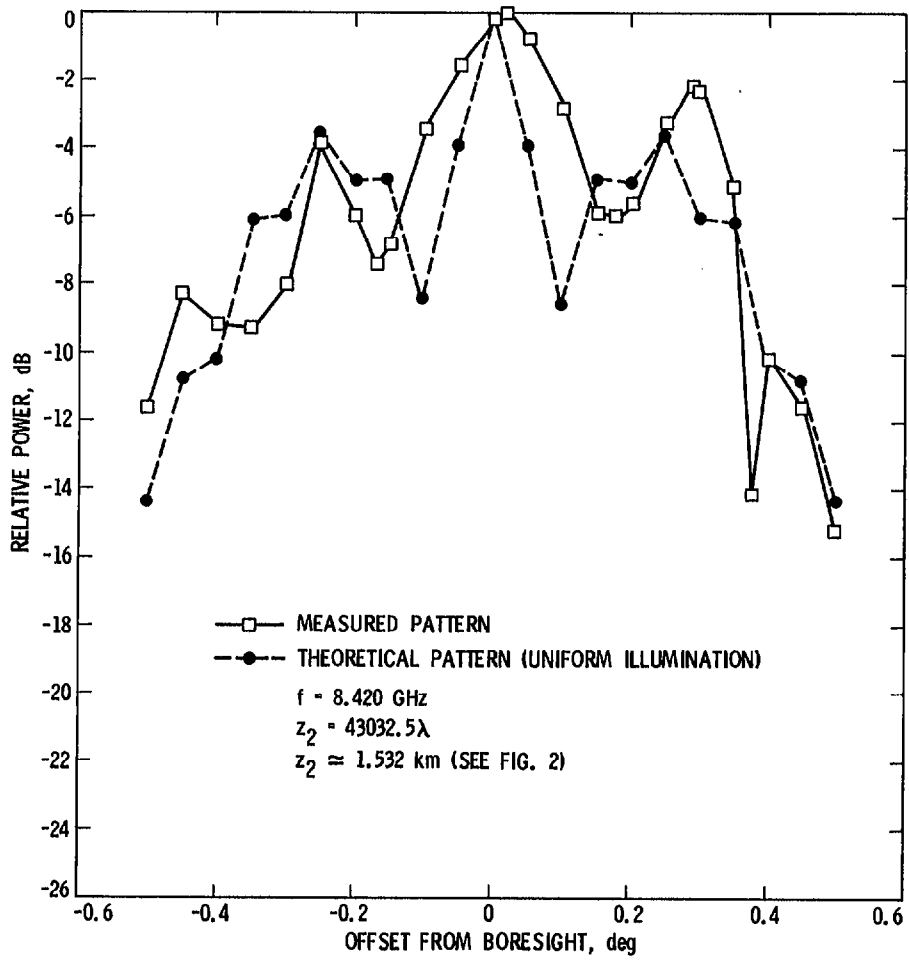


Fig. 6. 25-m-dia. antenna and 1.83-m-dia. receive-reference antenna at DSS 13. The S-band feed of the 1.83-m-dia. antenna shown in photograph was replaced by an X-band feed



**Fig. 7. Received power vs offset angle scanning in the elevation angle plane at 8.420 GHz when the 26-m paraboloidal antenna was located 1.53 km distance from the 1.83-m-dia. transmit (collimation tower) antenna**